31st Annual International Conference of the IEEE EMBS
Minneapolis, Minnesota, USA, September 2-6, 2009

Estimation of the Aortic Pressure Waveform from a Radial Artery Pressure Waveform via an Adaptive Transfer Function: Feasibility Demonstration in Swine

Gokul Swamy, *Student Member, IEEE*, Da Xu, *Student Member, IEEE* and Ramakrishna Mukkamala, *Member, IEEE*

Abstract—**We previously proposed a new technique to estimate the physiologically and clinically more relevant central aortic pressure (AP) waveform from a conveniently and safely measured peripheral artery pressure (PAP) waveform distorted by wave reflections. In contrast to conventional generalized transfer function (GTF) techniques, the technique is able to adapt the transfer function relating PAP to AP to the inter-patient and temporal variability of the arterial tree by defining it through a tube model and invoking the fact that aortic flow is negligible during diastole to estimate the unknown model parameters. We conducted feasibility testing of this adaptive transfer function technique here with respect to radial artery pressure (RAP) waveforms, for the first time, as well as femoral artery pressure (FAP) waveforms from four swine instrumented with AP catheters during several hemodynamic conditions. Our results showed that the AP waveforms estimated by the technique from the RAP and FAP waveforms were in superior agreement to the measured AP waveforms (overall respective errors of 4.1 and 4.8 mmHg) than the two unprocessed PAP waveforms (9.1 and 8.1 mmHg) and a previous GTF technique trained on a subset of the same data (5.0 and 5.8 mmHg).**

I. Introduction

It is well recognized that the central aortic pressure (AP) waveform generally carries greater physiologic significance than peripheral artery pressure (PAP) waveforms distorted by wave reflections. Further, centrally measured arterial pressures have been shown to offer superior clinical information to corresponding measurements made in more peripheral arteries [1, 2]. Nevertheless, PAP waveforms are much more commonly measured in clinical practice due to the relative ease and safety of their measurement.

As a result, a number of techniques have been proposed to estimate the AP waveform from measured PAP waveforms (e.g., [3-5]). The common assumption of almost all of these techniques is that a single, universal or generalized transfer function (GTF) exists that can accurately transform a PAP waveform, especially from the upper limb, into the AP waveform of all patients over all time. However, an ideal technique would be able to adapt the mathematical transformation from PAP to AP to the inter-patient and temporal variability of the arterial tree.

A short time ago, we developed perhaps the first fully adaptive technique to estimate the AP waveform by exploiting the commonality in multiple PAP waveforms via multi-channel blind system identification (MBSI) [6, 7]. We applied this MBSI technique to the radial and femoral artery pressure (RAP and FAP) waveforms from four swine during several hemodynamic conditions, and the estimated AP waveforms showed superior agreement to simultaneously measured AP waveforms than the two unprocessed PAP waveforms and a previous GTF technique. However, the disadvantage of this technique is the requirement of more than one PAP waveform for measurement.

More recently, we conceived another fully adaptive technique to estimate the AP waveform but this time from just a single PAP waveform via a tube model-based transfer function whose unknown parameters are estimated by capitalizing on pre-knowledge of aortic *flow* [8]. We likewise showed the feasibility of this adaptive transfer function (ATF) technique with respect to FAP waveforms from six dogs over a much broader range of hemodynamic conditions.

In this study, we aimed to demonstrate the feasibility of the ATF technique with respect to more commonly measured RAP waveforms. To achieve this aim, we applied the ATF technique to the aforementioned swine RAP waveforms as well as the corresponding FAP waveforms. In this way, we were also able to directly compare the estimated AP waveforms with those previously obtained by our MBSI technique and a GTF technique.

II. Methods

A. Adaptive Transfer Function (ATF) Technique

Our ATF technique is described in detail elsewhere [8]. We review the technique at a conceptual level below.

The Figure illustrates the ATF technique. As shown in the left panel of this figure, the arterial tree is modeled as a parallel combination of m uniform wave propagation tubes terminated by lumped loads. The i^{th} tube represents the path from the aorta to the i^{th} peripheral artery. As supported by Poiseulle's law, each tube is frictionless and therefore has constant characteristic impedance ($Z_{ci} = \sqrt{(l_i/c_i)}$, where l_i and c_i are the total inertance and compliance of the tube) and allows waves to propagate with constant delay time from one end of the tube to the other ($T_{di} = \sqrt{(l_i c_i)}$). The i^{th} terminal load represents the arterial bed distal to the i^{th} peripheral artery.

Manuscript received April 7, 2009. This work was supported by the National Science Foundation (CAREER 0643477).

G. Swamy is with the Department of Electrical and Computer Engineering, Michigan State University, East Lansing, MI 48824, USA (e-mail: swamygok@msu.edu).

D. Xu is with the Department of Electrical and Computer Engineering, Michigan State University, East Lansing, MI 48824, USA (e-mail: xuda@msu.edu).

R. Mukkamala is with the Department of Electrical and Computer Engineering, Michigan State University (phone: 517-353-3120; fax: 517-353-1980; e-mail: rama@egr.msu.edu).

Consistent with previous tube model studies [5], each terminal load has a frequency-dependent impedance ($Z_i(\omega)$) characterized by a pole and zero (at $-A_i$ and $-B_i$) that are dependent on the peripheral resistance and compliance as well as a gain factor equal to the characteristic impedance of the corresponding tube (i.e., Z_{ci}).

According to this model, a PAP waveform ($p_{pi}(t)$) is related to the AP waveform ($p_a(t)$) through the transfer function shown in the upper, right panel of the Figure. Thus, this pressure→pressure transfer function could be applied to $p_{pi}(t)$ so as to determine $p_a(t)$, if its three model parameters, T_{di}, A_i, and B_i, were known.

To this end, T_{di} is first measured non-invasively with, for example, a handheld tonometer placed on a superficial artery near the heart [5]. Only one such T_{di} measurement is made for a given subject during a monitoring period (e.g., days to weeks), as l_i and c_i may not greatly vary over this time period.

The three parameters are then estimated from the measured $p_{pi}(t)$ and initial T_{di} value by exploiting the fact that aortic flow is negligible during each diastolic interval provided that aortic regurgitation is absent. Thus, as indicated in the left panel of the Figure, the arterial flow at each tube entrance in the arterial tree model (arterial entry flow) may likewise be small during these time intervals. In particular, according to this model, $p_{pi}(t)$ is related to the arterial entry flow waveform to the corresponding peripheral artery ($q_{ai}(t)$) through the transfer function shown in the lower, right panel of the Figure. This pressure→flow transfer function has the same unknown model parameters as the pressure→pressure transfer function. The common parameters are estimated by finding the pressure→flow transfer function, which when applied to $p_{pi}(t)$, minimizes the energy of the $q_{ai}(t)$ (scaled by Z_{ci}) output over its diastolic intervals. In other words, as shown in the lower, right panel of the Figure, the parameters are determined so as to optimally map $p_{pi}(t)$ to $q_{ai}(t)$ of zero during diastole.

Finally, the pressure→pressure transfer function with the estimated model parameters is applied to $p_{pi}(t)$ to estimate $p_a(t)$. This transfer function is adaptive by virtue of periodically re-estimating the model parameters.

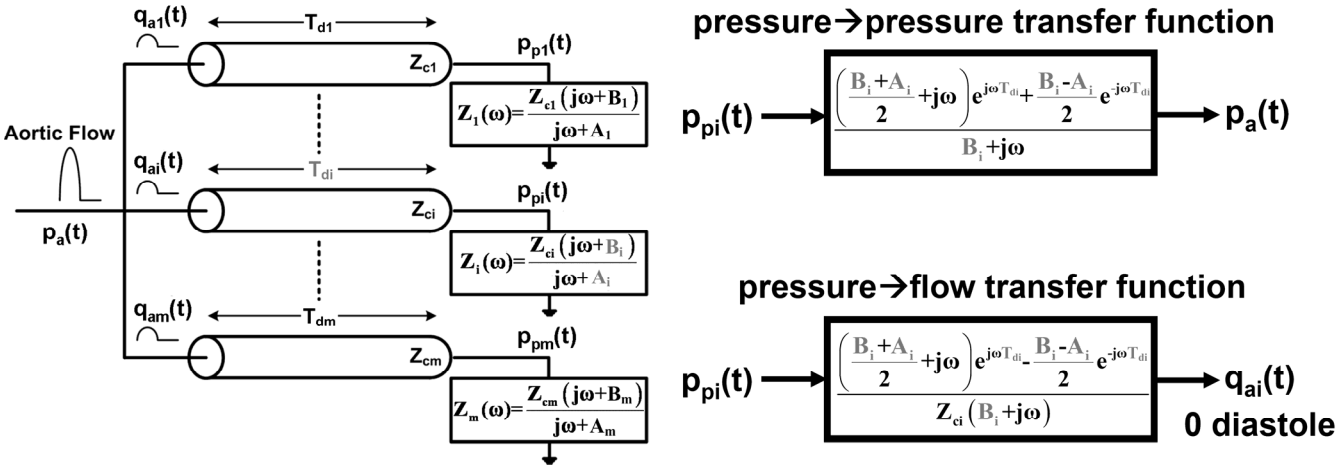

Fig. Adaptive transfer function (ATF) technique for estimating the aortic pressure (AP) waveform from a peripheral artery pressure (PAP) waveform. Gray indicates model parameters for estimation. See text for remaining details.

B. Swine Data Analysis

To demonstrate feasibility of the ATF technique with respect to RAP waveforms, we analyzed previously collected swine data. These data are also described in detail elsewhere [6, 7]. Briefly, the data include RAP and FAP waveforms (via fluid-filled catheters) and the reference AP waveform (via a high fidelity, micromanometer-tipped catheter) from four anesthetized swine (30-34 kg) during infusions of volume, phenylephrine, dobutamine, isoproterenol, esmolol, nitroglycerin, and acetylcholine.

We specifically applied the ATF technique to each 15-second segment of the swine RAP and FAP waveforms, with T_{di} measured for each animal as the time interval between the onsets of upstroke of the initial beats of the AP and PAP waveforms. We quantitatively evaluated the estimated AP waveforms with respect to the measured AP waveforms in terms of the sample-to-sample root-mean-squared-error (RMSE). We then compared the RMSEs with the corresponding RMSEs of the unprocessed RAP and FAP waveforms (after time alignment to account for the delay) as well as the AP waveforms estimated by our MBSI technique and an autoregressive exogenous input-based GTF technique [4] trained on a subset of the swine data. All of these latter, comparative results have been previously reported [7].

III. Results

The Table shows the RMSEs of the AP waveforms estimated by the ATF technique from the RAP and FAP waveforms for each animal and overall. This table also includes the previously reported, corresponding RMSEs of the time aligned PAP waveforms and the AP waveforms estimated by our MBSI technique and the previous GTF technique.

The overall RMSEs of the unprocessed RAP and FAP waveforms with respect to the reference AP waveforms were 9.1 and 8.1 mmHg, respectively. All three techniques were able to estimate the AP waveform with greater accuracy than simply time aligning the PAP waveforms. As might be expected, the MBSI technique, which analyzed the RAP and FAP waveforms at once, was most accurate with an overall RMSE of 3.5 mmHg. The ATF technique, which analyzed the RAP and FAP waveforms one at a time, was next in accuracy with respective overall RMSEs of 4.1 and 4.8 mmHg. The GTF technique, which also separately analyzed the two PAP waveforms, was least accurate with corresponding RMSEs of 5.0 and 5.8 mmHg, even though it had the distinct advantage over the two adaptive techniques of being trained on a subset of the swine data. Note that the improved AP waveform estimation from the RAP waveforms over the FAP waveforms achieved by both the ATF and GTF techniques is likely due to apparent damping in a portion of the FAP waveform from one of the animals.

TABLE

ROOT-MEAN-SQUARED-ERROR (RMSE) OF THE UNPROCESSED RADIAL AND FEMORAL ARTERY PRESSURE (RAP AND FAP) WAVEFORMS AND THE AP WAVEFORMS ESTIMATED BY THE ADAPTIVE TRANSFER FUNCTION (ATF) TECHNIQUE, A PREVIOUS GENERALIZED TRANSFER FUNCTION (GTF) TECHNIQUE, AND OUR PREVIOUS MULTI-CHANNEL BLIND SYSTEM IDENTIFICATION (MBSI) TECHNIQUE.

Animal	Unprocessed PAP RMSE [mmHg]		ATF RMSE [mmHg]		GTF RMSE [mmHg]		MBSI RMSE [mmHg]
	RAP	FAP	RAP	FAP	RAP	FAP	
1	4.0	11.6	2.7	3.9	4.2	4.8	2.5
2	10.5	7.8	3.5	2.9	4.6	5.2	3.9
3	9.4	6.3	2.7	6.9	6.0	6.9	3.4
4	9.3	7.0	6.7	4.3	5.1	5.6	3.4
Total	9.1	8.1	4.1	4.8	5.0	5.8	3.5

IV. DISCUSSION

In summary, we recently introduced a new technique to estimate the AP waveform from a single PAP waveform. In contrast to conventional GTF techniques, the technique is able to adapt the transfer function relating PAP to AP to the inter-patient and temporal variability of the arterial tree by defining it through a tube model and invoking the fact that aortic flow is negligible during diastole to estimate the unknown model parameters. We tested this ATF technique here with respect to RAP waveforms, for the first time, as well as FAP waveforms from four swine during several hemodynamic conditions. Our results generally demonstrated feasibility of the technique with respect to RAP waveforms as well as FAP waveforms. In particular, the technique was able to significantly reduce the wave distortion in both the RAP and FAP waveforms and estimate the AP waveform from both of these PAP waveforms with equally greater accuracy over a previous GTF technique trained on a subset of the same data. Our previous MBSI technique did estimate the AP waveforms more accurately than the ATF technique, especially during arterial line damping. However, the trade-off for the improved performance afforded by this likewise adaptive technique is the need for an additional PAP waveform measurement.

We are currently seeking to improve the accuracy of the ATF technique by, for example, employing a more detailed model of the terminal load that accounts for peripheral inertance. We are also planning to conduct studies to evaluate the ATF technique as well as the MBSI technique in humans. Ultimately, this line of research may translate to more precise arterial pressure monitoring and titration of therapy in surgery and critical care patients with PAP catheters already in place as well as in other patient populations with commercially available, non-invasive PAP sensors.

REFERENCES

[1] M. E. Safar, J. Blacher, B. Pannier, A. P. Guerin, S. J. Marchais, P. Guyonvarc'h, and G. M. London, "Central pulse pressure and mortality in end-stage renal disease," *Hypertension*, vol. 39, pp. 735-738, 2002.

[2] T. K. Waddell, A. M. Dart, T. L. Medley, J. D. Cameron, and B. A. Kingwell, "Carotid pressure is a better predictor of coronary artery disease severity than brachial pressure," *Hypertension*, vol. 38, pp. 927-931, 2001.

[3] M. Karamanoglu, M. F. O'Rourke, A. P. Avolio, and R. P. Kelly, "An analysis of the relationship between central aortic and peripheral upper limb pressure waves in man," *Eur. Heart J.*, vol. 14, pp. 160-167, 1993.

[4] B. Fetics, E. Nevo, C. H. Chen, and D. A. Kass, "Parametric model derivation of transfer function for noninvasive estimation of aortic pressure by radial tonometry," *IEEE Trans. Biomed. Eng.*, vol. 46, no. 6, pp. 698-706, 1999.

[5] M. Sugimachi, T. Shishido, K. Miyatake, and K. Sunagawa, "A new model-based method of reconstructing central aortic pressure from peripheral arterial pressure," *Jpn. J. Physiol.*, vol. 51, no. 2, pp. 217-222, 2001.

[6] G. Swamy, Q. Ling, T. Li, and R. Mukkamala, "Blind identification of the aortic pressure waveform from multiple peripheral artery pressure waveforms," *Am. J. Physiol.*, vol. 292, no. 5, pp. H2257-H2264, 2007.

[7] G. Swamy and R. Mukkamala, "Estimation of the aortic pressure waveform and beat-to-beat cardiac output from multiple peripheral artery pressure waveforms," *IEEE Trans. Biomed. Eng.*, vol. 55, pp. 1521-1529, 2008.

[8] G. Swamy, R. Mukkamala, and N. B. Olivier, "Estimation of the aortic pressure waveform from a peripheral artery pressure waveform via an adaptive transfer function," *Proc. 30th Annual IEEE EMBS Conf.*, vol. 1, pp. 1385-1388, 2008.